Biobased Copolymers *via* Cationic Ring-Opening Copolymerization of Levoglucosan Derivatives and ε-Caprolactone

Mayuri K. Porwal[a], Christopher J. Ellison[a]*, Theresa M. Reineke[b]*

[a] Department of Chemical Engineering and Materials Science, University of Minnesota, Minneapolis, Minnesota 55455, United States

[b] Department of Chemistry, University of Minnesota, Minneapolis, Minnesota 55455, United States

Email: porwa001@umn.edu

*Corresponding authors

Email: cellison@umn.edu, treineke@umn.edu

Abstract

Simultaneous ring-opening copolymerization is a powerful strategy for the synthesis of highly functional copolymers from different types of cyclic monomers. Although copolymers are essential to the plastics industry, environmental concerns associated with the current fossil-fuel based synthetic polymers have led to an increasing interest in the use of renewable feedstock for copolymer synthesis. Herein, we report a scalable synthetic platform to afford unique polysaccharides with different pendant functional groups from biomass-derived levoglucosan and ε-caprolactone *via* cationic ring-opening copolymerization (cROCOP). Biocompatible and recyclable bismuth triflate was identified as the optimal catalyst for cROCOP of levoglucosan. Copolymers from tribenzyl levoglucosan and ε-caprolactone, as well as from tribenzyl and triallyl levoglucosan were successfully synthesized. The tribenzyl levoglucosan monomer composition ranged from 16 % to 64 % in the copolymers with ε-caprolactone, and 22 % to 79 % in the copolymers with triallyl levoglucosan. The allylic levoglucosan copolymer can be utilized as a renewably-derived scaffold to modify copolymer properties and create other polymer architectures *via* post-polymerization modification. Monomer reactivity ratios were determined to investigate the copolymer microstructure, indicating that levoglucosan-based copolymers have a gradient architecture. Additionally, we demonstrated that the copolymer glass transition temperature (T_g, ranging from −44.3 °C to 33.8 °C), thermal stability, and crystallization behavior could be tuned based on the copolymer composition. Overall, this work underscores the utility of levoglucosan as a bioderived feedstock for the development of functional sugar-based copolymers with applications ranging from sustainable materials to biomaterials.

TOC Graphic

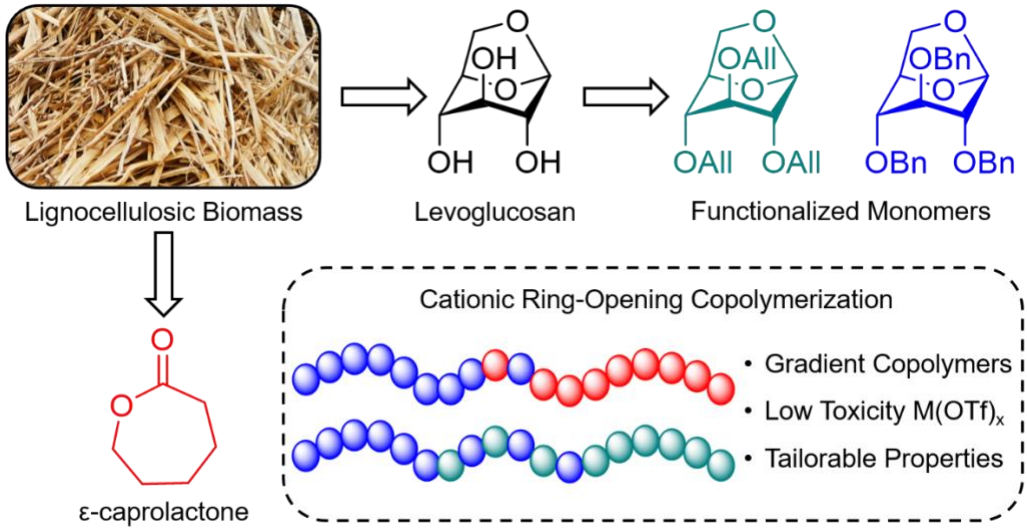
Lignocellulosic Biomass
Levoglucosan
Functionalized Monomers
OH
OH
OH
OAll
OAll
OAll
OBn
OBn
OBn
ε-caprolactone
Cationic Ring-Opening Copolymerization
• Gradient Copolymers
• Low Toxicity M(OTf)x
• Tailorable Properties

Simultaneous ring-opening copolymerization is a promising and powerful strategy for the synthesis of highly functional and tailorable copolymers from an extensive class of cyclic monomers.[1–5] Copolymers are commercially relevant and essential to the plastics industry due to their unique comonomer-sequence dependent properties,[6] however, most of the current synthetic polymers are derived from fossil fuels, prompting severe environmental concerns.[7] To address these issues, an increasing number of recent investigations are focused on employing renewable feedstocks, particularly those derived from lignocellulosic biomass, for the synthesis of sustainable polymeric materials.[8,9] Levoglucosan (Scheme 1A) is an interesting and relatively untapped renewable feedstock that can be obtained directly from the fast pyrolysis of cellulosic biomass in high yields (80 %) and at a competitive price point with current petroleum derived feedstocks.[10–12] Levoglucosan is an anhydro sugar containing a bicyclic acetal linkage that is amenable to cationic ring-opening polymerization (cROP).[13] Furthermore, the three hydroxyl groups on levoglucosan can be easily synthetically modified both pre- and post- polymerization to install a variety of pendant groups for tailored properties. Consequently, levoglucosan is an attractive feedstock for the synthesis of sugar-based copolymers *via* cationic ring-opening copolymerization (cROCOP) with other renewable cyclic monomers.

The cROCOP of a tribenzyl levoglucosan monomer (Scheme 1A, **1**) was first reported more than 50 years ago, typically in combination with other protected levoglucosan derivatives or protected levoglucosan isomers as comonomers.[14–20] In these previous studies, the cROCOP of levoglucosan derivatives was performed at very low temperatures (−60 °C), and with the highly toxic and difficult-to-handle initiator PF_5.[14–21] Moreover, very limited work has been done to copolymerize levoglucosan with different types of cyclic monomers other than anhydro sugars. Uryu *et.al.* copolymerized tribenzyl levoglucosan (**1**) with dioxolane and epichlorohydrin in the

presence of PF_5 at −60 °C and obtained blocky and gradient copolymers, respectively.[22] However, to the best of our knowledge, this is the only example of cROCOP of levoglucosan with other types of cyclic monomers. Indeed, there is ample space for the development and characterization of functional levoglucosan-based copolymers and improving the fundamental understanding and activity of copolymerization with chemically-different monomers.

ε-caprolactone (Scheme 1A, **3**) is a promising cyclic ester monomer for cROCOP with levoglucosan that can be synthesized from 5-hydroxymethyl furfural – a lignocellulosic biomass-based platform chemical.[9] The homopolymer of **3**, polycaprolactone, is a commercially produced polyester with widespread applications in the fields of drug delivery, tissue engineering, medical devices, sutures, etc.[9,23] The cROCOP of levoglucosan with ε-caprolactone will enable facile access to acetal-ester polysaccharides with potential as biomaterials for applications such as drug delivery, tissue engineering, gene therapy, etc.[23,24] Additionally, the incorporation of levoglucosan and ε-caprolactone in a gradient or blocky fashion will enable access to fully biobased copolymers with hard and soft segments that can be utilized as thermoplastic elastomers (TPEs).[25,26] Notably, the cROCOP of cyclic acetals with cyclic esters has been the subject of a handful studies, where 1,3-dioxolane is commonly copolymerized with either ε-caprolactone or L-lactide.[27–31] Although these studies demonstrate successful formation of an acetal-ester copolymer, monomer reactivity ratios are not determined for the assessment of copolymer microstructure. Taken together, these factors have led us to explore the cROCOP of levoglucosan and ε-caprolactone with low toxicity polymerization catalysts to obtain novel sugar-based copolymers.

Herein, we report a scalable synthetic platform to afford unique polysaccharides with different pendant functional groups derived from levoglucosan and ε-caprolactone (Scheme 1). To identify alternatives to PF_5, low toxicity metal triflate catalysts were screened for the cROCOP of

levoglucosan-based benzyl (Bn) **1** and allyl (All) **2** functional monomers (Scheme 1A) with ε-caprolactone **3**. Bismuth triflate—which is a biocompatible and recyclable catalyst—was identified as a promising candidate to synthesize levoglucosan-based copolymers. A series of copolymers with different compositions were prepared to access a wide range of thermal properties based on the copolymer composition and levoglucosan pendant groups. Lastly, monomer reactivity ratios were determined to assess the copolymer microstructure revealing a gradient architecture for levoglucosan-based copolymers. This work lays the foundation for fundamental synthesis and development of levoglucosan as a biobased platform chemical to afford sugar-based copolymers with pendant functional groups for applications ranging from sustainable TPEs to biomaterials.

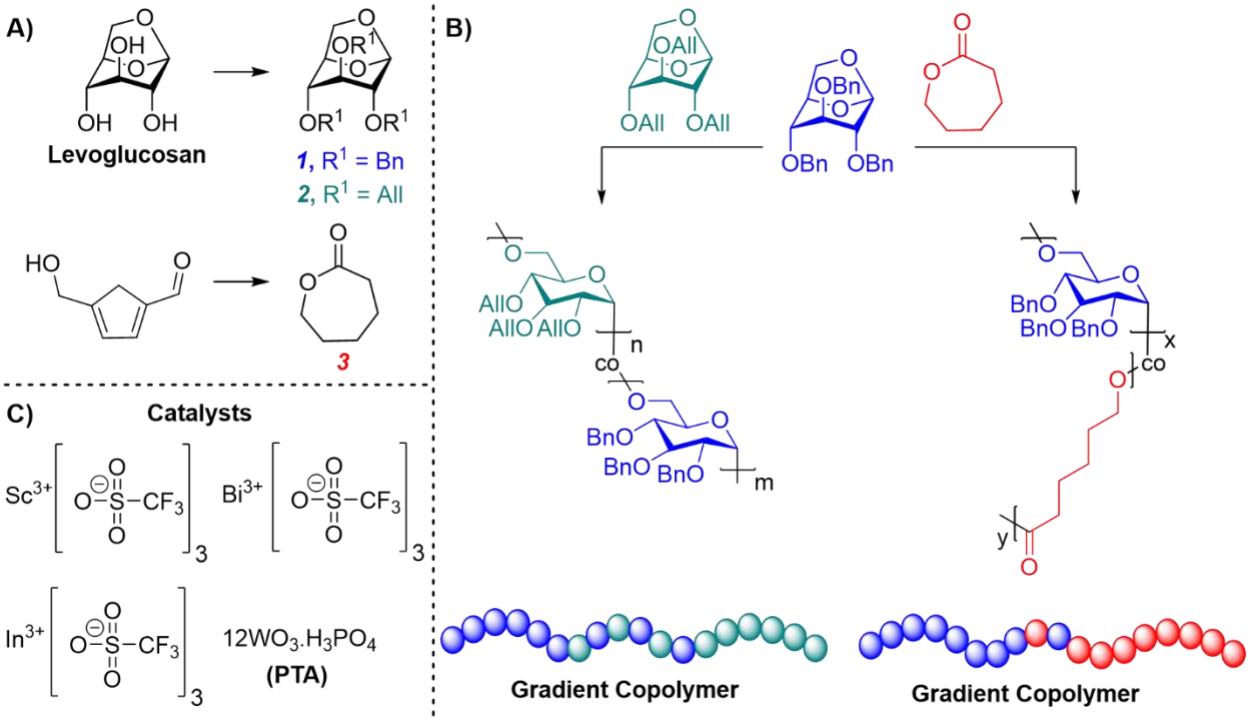

Scheme 1. A) Chemical structures of monomers used in this study. B) Schematic depicting synthesis of copolymers via cROCOP of **1**/**2** and **1**/**3** respectively. C) Chemical structures of polymerization catalysts used in this study for cROCOP.

Monomer **1** was purchased from a commercial supplier and monomer **2** was synthesized on a multigram scale as previously reported.[32] Four commercially available polymerization catalysts were screened for the cROCOP of **1**, **2**, and **3** (Scheme 1C) due to their efficiency in ring

opening cyclic acetals, such as levoglucosan, as demonstrated in earlier studies,[13,32,33] as well as their ability to ring open cyclic esters like ε-caprolactone.[34,35] To understand the effect of catalyst type, catalyst loading, and monomer feed ratio, a library of polymerization experiments was performed and the results are summarized in Tables 1 and 2. The screening studies for the cROCOP of **1** and **3** at a 50 : 50 feed ratio of **1** : **3** revealed that all catalysts except $In(OTf)_3$ were successful in producing poly(**1**-co-**3**) with up to 50% incorporation of **1** in the copolymer (Table 1, entries 1-4). Further studies were performed at lower catalyst loadings to target higher molecular weights (Table 1, entries 5-7), and these studies demonstrated $Bi(OTf)_3$ to be the optimal catalyst for cROCOP of **1** and **3** (Table 1, entry 6) resulting in poly(**1**-co-**3**) with an M_n of 10.4 kDa and low dispersity of 1.1. Subsequent cROCOP of **1** and **3** with $Bi(OTf)_3$ at non-stoichiometric feed ratios of **1** : **3** resulted in copolymers with M_n ranging from 7.2 to 11.7 kDa and low dispersities (Table 1, entries 8-11). Overall, through the $Bi(OTf)_3$ catalyzed copolymerization of **1** and **3**, a series of poly(**1**-co-**3**) copolymers were successfully synthesized with copolymer composition of **1** ranging from 16% to 64%.

Table 1. Summary of cROCOP of **1** and **3** under various polymerization conditions. All polymerizations were performed in CH_2Cl_2 at room temperature for 72 h. [a]Monomer conversion determined by ^1H NMR spectroscopy. [b]Molecular weight and dispersity determined by SEC-MALS in DMF. [†]Samples obtained from reactivity ratio analysis experiments.

No	Catalyst	**1** : **3**	**1** : **Cat**	Conversion[a] (%)	M_n^b (kDa)	$Đ^b$	F_1 (%)	F_3 (%)
1	$Sc(OTf)_3$	1 : 1	50 : 1	**1** = 56 ; **3** = 78	6.2	1.1	50	50
2	$Bi(OTf)_3$	1 : 1	50 : 1	**1** = 85 ; **3** > 99	5.6	1.3	50	50
3	$In(OTf)_3$	1 : 1	50 : 1	**1**= 73 ; **3** = 83	Bimodal	-	-	-
4	PTA	1 : 1	50 : 1	**1** = 99 ; **3** > 99	4.0	1.4	35	65
5	$Sc(OTf)_3$	1 : 1	200 : 1	**1** = 0 ; **3** = 27	-	-	-	-
6	$Bi(OTf)_3$	1 : 1	200 : 1	**1**= 35 ; **3** = 95	10.4	1.1	16	84

7	PTA	1 : 1	200 : 1	**1** = 80 ; **3** > 99	5.9	1.4	27	73
8	$Bi(OTf)_3$	3 : 1	200 : 1	**1** = 78 ; **3** > 99	7.8	1.3	49	50
9	$Bi(OTf)_3$	1 : 3	67 : 1	**1** = 74 ; **3** > 99	11.7	1.2	18	82
10†	$Bi(OTf)_3$	3 : 1	100 : 1	**1** = 75 ; **3** > 99	7.2	1.4	64	36
11†	$Bi(OTf)_3$	1 : 3	34 : 1	**1** = 84 ; **3** > 99	8.1	1.2	27	73

Table 2. Summary of cROCOP of **1**, **2** and **3** under various polymerization conditions. All polymerizations were performed in CH_2Cl_2 at room temperature for 72 h. [a]Monomer conversion determined by ^1H NMR spectroscopy. [b]Molecular weight and dispersity determined by SEC-MALS in DMF. †Samples obtained from reactivity ratio analysis experiments. *Sample could not be precipitated in methanol for SEC-MALS. #A mixture of homopolymers poly**2** and poly**3** based on DOSY NMR analysis.

No	M1	M2	Catalyst	M1 : M2	M1 : Cat	Conversion[a] (%)	M_n^b (kDa)	$Đ^b$	F_{M1} (%)	F_{M2} (%)
1	**1**	**2**	$Sc(OTf)_3$	1 : 1	50 : 1	**1** = 45 ; **2** = 80	5.9	1.5	42	58
2	**1**	**2**	$Bi(OTf)_3$	1 : 1	50 : 1	**1** = 41 ; **2** = 76	6.3	1.2	42	58
3	**1**	**2**	PTA	1 : 1	50 : 1	**1** = 0 ; **2** = 0	-	-	-	-
4*	**1**	**2**	$In(OTf)_3$	1 : 1	50 : 1	**1** = 24 ; **2** = 47	-	-	-	-
5*	**1**	**2**	$Bi(OTf)_3$	1 : 1	100 : 1	**1** = 19 ; **2** = 50	-	-	-	-
6	**1**	**2**	$Bi(OTf)_3$	1 : 1	200 : 1	**1** = 0 ; **2** = 0	-	-	-	-
7	**1**	**2**	$Bi(OTf)_3$	3 : 1	50 : 1	**1** = 70 ; **2** = 65	5.4	1.5	65	35
8	**1**	**2**	$Bi(OTf)_3$	1 : 3	17 : 1	**1** = 54 ; **2** = 87	6.9	1.6	22	78
9†	**1**	**2**	$Bi(OTf)_3$	3 : 1	34 : 1	**1** = 90 ; **2** = 95	5.8	1.6	79	21
10†	**1**	**2**	$Bi(OTf)_3$	1 : 3	11 : 1	**1** = 86 ; **2** = 96	15.4	1.7	27	73
11	**2**	**3**	$Sc(OTf)_3$	1 : 1	50 : 1	**2** = 11 ; **3** = 58	Bimodal	-	-	-
12	**2**	**3**	$Bi(OTf)_3$	1 : 1	50 : 1	**2** = 0 ; **3** = 72	-	-	-	-
13#	**2**	**3**	$In(OTf)_3$	1 : 1	50 : 1	**2** = 88 ; **3** > 99	17.3	1.6	30	70
14	**2**	**3**	PTA	1 : 1	50 : 1	**2** = 88 ; **3** > 99	Bimodal	-	-	-

When the cROCOP of **1** and **2** at a 50 : 50 feed ratio of **1** : **2** was performed with the different catalysts (Table 2, entries 1-4), we found that only $Sc(OTf)_3$ and $Bi(OTf)_3$ yielded poly(**1**-co-**2**) with 42% incorporation of **1**, with $Bi(OTf)_3$ resulting in slightly higher M_n and lower dispersities under comparative conditions. Similar to previous screening studies, further experiments were performed at lower $Bi(OTf)_3$ loadings to target poly(**1**-co-**2**) with higher M_n. However, it was found that at $Bi(OTf)_3$ loadings < 2 mol% low or zero conversion of **1** was achieved (Table 2, entries 5 and 6). It is hypothesized that a minimum catalyst loading of 1 mol% is required to initiate the cROCOP of **1** and **2**, likely due to the non-productive coordination of Bi with the allylic/benzylic ether oxygens and the glucopyranose ring oxygen, as reported in our previous study.[32] It is possible that "extra" catalyst is needed to overcome the nonproductive coordination effects discussed above and successfully initiate the copolymerization of **1** and **2**.[32] Moreover, similar high catalyst loadings were reported in earlier studies involving cROCOP of **1** with other protected levoglucosan derivatives.[14–20] Nevertheless, a range of poly(**1**-co-**2**) copolymers were synthesized with $Bi(OTf)_3$ at different feed ratios of **1** : **2** with M_n varying from 5.4 to 15.4 kDa and copolymer composition of **1** ranging between 22% and 79% (Table 2, entries 7-10).

Finally, the cROCOP of **2** and **3** at a 50 : 50 feed ratio of **2** : **3** was also attempted with the different catalysts (Table 2, entries 11-14), and the results show that only $In(OTf)_3$ and PTA were successful in initiating the polymerization of **2** and **3** at high monomer conversions. SEC analysis of the obtained polymers revealed that the PTA catalyzed sample had a bimodal SEC distribution likely suggesting the presence of two homopolymers instead of a copolymer (Figure S20, dotted line). SEC analysis of the $In(OTf)_3$ catalyzed sample revealed a monomodal but broad molecular weight distribution (Figure S20, solid line). To investigate whether the broad molecular weight

distribution was due to the presence of two homopolymers, the sample was subjected to diffusion-ordered NMR spectroscopy (DOSY). DOSY analysis (Figure S21) demonstrated a broad and tailing diffusion coefficient peak with distinct signals for monomers **2** and **3**, likely indicating the presence of homopolymers poly**2** and poly**3** instead of poly(**2**-co-**3**). These results demonstrate that **2** and **3** are incompatible as comonomers for cROCOP, potentially due to drastic homopolymerization kinetic differences between **2** and **3** (Table S1).[32] It is noteworthy that the levoglucosan pendant group identity can drastically affect cROCOP amenability, and this will be investigated further in future studies with other levoglucosan-derived monomers. Nonetheless, to summarize, the library of cROCOP experiments and corresponding SEC analysis showed successful synthesis of poly(**1**-co-**3**) and poly(**1**-co-**2**) with a wide range of incorporation of **1** in both the copolymers along with moderate M_n and dispersities.

The representative ^{1}H NMR spectra of the purified poly(**1**-co-**3**) and poly(**1**-co-**2**) copolymers are shown in figure 1A and 1B, respectively, with the corresponding peaks from each monomer numbered and assigned further suggesting successful copolymer formation. The detailed ^{1}H NMR analysis for determining conversion of each monomer and % incorporation of each monomer in the final copolymer is described in sections 3 and 4 of the Supplementary Information, respectively. ^{1}H NMR analysis of poly(**1**-co-**2**) also indicates that the alkene functionality in the copolymer is intact after cROCOP with the allyl proton resonances at 5.91 ppm, 5.24 ppm, and 5.09 ppm. In our previous study we demonstrated that the multiple allylic pendant groups on the homopolymer poly**2** could be readily subjected to post-polymer modification.[32] Similarly, the allylic pendant groups of poly(**1**-co-**2**) copolymer can be subjected to post-polymerization modification to further tailor polymer properties and access other interesting polymer architectures such as amphiphilic copolymers.

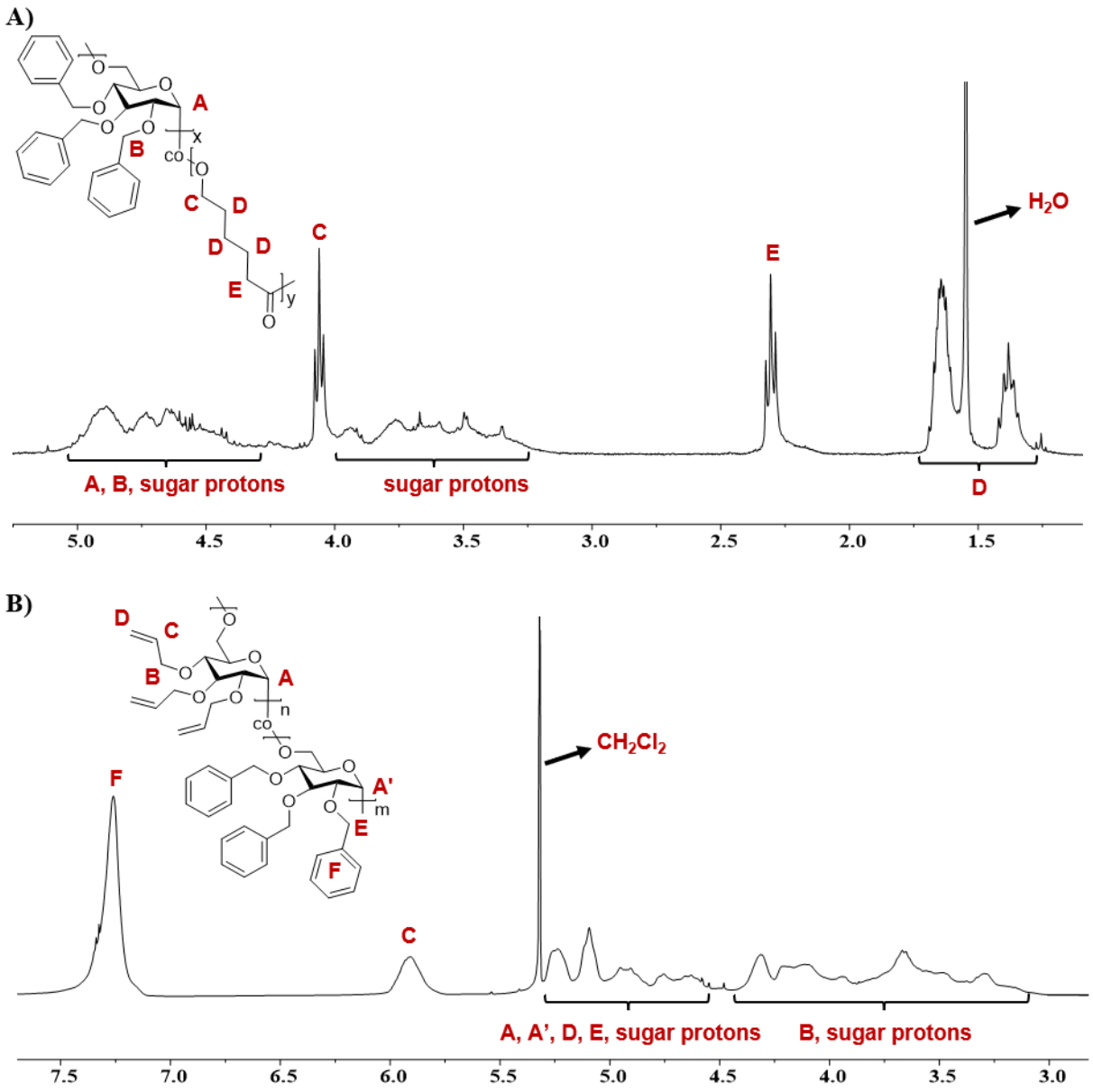

Figure 1. ^{1}H NMR spectra of the synthesized A) poly(**1**-co-**3**) from Table 1 entry 8, and B) poly(**1**-co-**2**) from Table 2 entry 2.

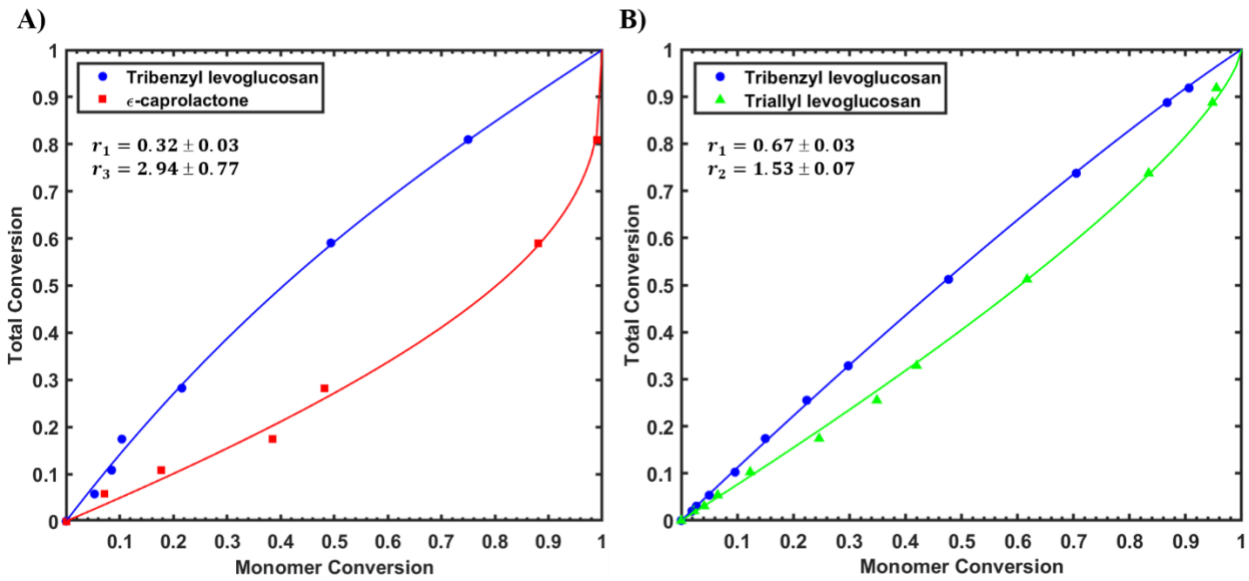

Figure 2. A) Reactivity ratio analysis for poly(**1**-co-**3**). Total polymerization conversion plotted against monomer conversion: (●) tribenzyl levoglucosan and (■) ε-caprolactone. Solid blue and red lines represent fits to the experimental data using the BSL model, eqs. 2 and 3, and the initial compositions: n_1 = 0.75 and n_3 = 0.25. B) Reactivity ratio analysis for poly(**1**-co-**2**). Total polymerization conversion plotted against monomer conversion: (●) tribenzyl levoglucosan and (▲) triallyl levoglucosan. Solid blue and green lines represent fits to the experimental data using the BSL model, eqs. 2 and 3, and the initial compositions: n_1 = 0.75 and n_2 = 0.25.

Apart from determining the percent incorporation of each monomer in the copolymer, understanding the statistics of monomer addition in the copolymer is also crucial for elucidating structure-property relationships as a function of copolymer composition. Therefore, determining the reactivity ratios of a pair of monomers involved in copolymerization is important for a complete understanding of the polymer microstructure. In the copolymerization of any two monomers A and B, reactivity ratios r_A and r_B are used to distinguish between the four common types of copolymerization behaviors, namely random ($r_A = r_B = 1$), alternating ($r_A = r_B = 0$), gradient ($r_A < 1 < r_B$), and blocky ($r_A, r_B >> 1$).[36,37] Therefore, the reactivity ratios for the copolymerization of **1** and **3** as well as for the copolymerization of **1** and **2** were determined using the Beckingham-Sanoja-Lynd (BSL) model.[36,37] The BSL model is an integrated and non-terminal copolymerization model that describes the compositional drift in nonterminal copolymerizations.[36,37] A non-terminal copolymerization model such as BSL can help distinguish between gradient

and random copolymerization regimes. In general, in the case of ionic copolymerizations such as cROCOP, the rate of monomer incorporation does not strongly depend on the identity of the chain end (as assumed in a terminal model) but is instead primarily dependent on the chemistry of the monomers.[38] This is because in the case of cROCOP the monomer incorporation statistics are dictated by the interaction of an incoming monomer with the cationic center, and this interaction is independent of the last monomer in the chain.[38] This type of copolymerization behavior is referred to as ideal or non-terminal copolymerization ($r_A \times r_B \approx 1$), and this characteristic suggests that the cROCOP of levoglucosan can be described by the BSL model.[38]

To determine the reactivity ratios for the different copolymerizations, the conversion for each monomer (p_A and p_B) was monitored over time, and the total monomer conversion (p_{AB}) was calculated using eqn. (1), where n_A and n_B are the initial mole fractions of A and B.[6] A plot of the total monomer conversion (p_{AB}) versus the individual monomer conversions (p_A and p_B) was then made and the resulting data was fit to eqs (2) and (3) to determine the reactivity ratios r_A and r_B.[6] To determine r_1 and r_3 for the copolymerization of **1** and **3**, a copolymerization kinetic study was performed (details in SI Section 4.1) at a **1** : **3** feed ratio of 75 : 25. The plot of total monomer conversion versus the individual monomer conversions and the corresponding BSL fits for poly(**1**-co-**3**) are depicted in figure 2A. The reactivity ratios were determined to be r_1 = 0.32 ± 0.03 and r_3 = 2.94 ± 0.77, indicating that the copolymerization of **1** with **3** results in a gradient copolymer. The product of the reactivity ratios is consistent with non-terminal copolymerization, i.e., $r_1 \times r_3 = 0.94$, as expected for an ionic copolymerization. These reactivity ratio values are consistent with the compositional drift observed during the experiment, with **3** being consumed earlier in the copolymerization. Furthermore, this analysis was repeated at a **1** : **3** feed ratio of 25

: 75 resulting in consistent reactivity ratios and a gradient characteristic for poly(**1**-co-**3**) (SI Section 4.1).

$$\text{Total Conversion } (p_{AB}) = 1 - n_A * (1 - p_A) - n_B * (1 - p_B) \quad \text{eqn. (1)}$$

$$p_{AB}\ (p_A) = 1 - n_A * (1 - p_A) - (1 - n_A) * (1 - p_A)^{r_B} \quad \text{eqn. (2)}$$

$$p_{AB}\ (p_B) = 1 - n_A * (1 - p_B)^{r_A} - (1 - n_A) * (1 - p_B) \quad \text{eqn. (3)}$$

Similarly, to determine r_1 and r_2 for the copolymerization of **1** and **2**, a copolymerization kinetic study was performed (details in SI Section 4.2) at a **1** : **2** feed ratio of 75 : 25. The plot of total monomer conversion versus the individual monomer conversions and the corresponding BSL fits for poly(**1**-co-**2**) are depicted in figure 2B. In this case the reactivity ratios were determined to be r_1 = 0.67 ± 0.03 and r_2 = 1.53 ± 0.07, and the product of reactivity ratios is again consistent with non-terminal copolymerization, i.e., $r_1 \times r_2 = 1.03$. These reactivity ratio values also indicate that the copolymerization of **1** with **2** results in a gradient copolymer. However, in comparison to the reactivity ratio values for poly(**1**-co-**3**), it is likely that the resultant comonomer sequence in poly(**1**-co-**2**) is a slight gradient as depicted in scheme 1B, due to the comparatively smaller difference between r_1 and r_2.[39] Finally, this analysis was also repeated at a **1** : **2** feed ratio of 25 : 75 again resulting in a gradient characteristic for poly(**1**-co-**2**) (SI Section 4.2). Overall, reactivity ratio analysis indicates a gradient microstructure for levoglucosan-based copolymers, due to which these copolymers could be important in a variety of applications ranging from biobased compatibilizers for immiscible polymer blends and TPEs to amphiphilic gradient copolymers for biomedical applications.[26]

The thermal properties of the levoglucosan-based copolymers were examined *via* differential scanning calorimetry (DSC) and thermogravimetric analysis (TGA) to understand thermal transitions and thermal stability, respectively. DSC thermograms for poly(**1**-co-**3**) are

shown in figure 3A and the corresponding data is summarized in figure 3E. DSC analysis shows that poly(**1**-co-**3**) copolymers with up to 25 % incorporation of **1** demonstrated melting (T_m) and crystallization transitions (T_c) indicating the presence of crystalline domains in the copolymers. Since poly**1** is completely amorphous (figure 3E), the crystalline regions in poly(**1**-co-**3**) are likely derived from CL homo-sequences, further supporting a gradient microstructure. DSC analysis of poly(**1**-co-**3**) with up to 25 % incorporation of **1** also revealed an interesting double melting peak which has been observed previously in other cyclic acetal-cyclic ester copolymers.[40,41] A potential explanation for this double melting phenomenon are the presence of lamellae with two different thicknesses.[42–44] The glass transition temperature (T_g) of poly(**1**-co-**3**) copolymers is between those of poly**1** and poly**3** homopolymers (figure 3A and 3E), with the T_g ranging from –44.3 °C to 21.5 °C when the copolymer composition changes from 16 % to 64 % incorporation of **1**. Similarly, the DSC thermograms for poly(**1**-co-**2**) are shown in figure 3B and the data is summarized in figure 3E. poly(**1**-co-**2**) copolymers are completely amorphous, and the T_g of the copolymers is between those of poly**1** and poly**2** homopolymers.

Lastly, the TGA curves for the native homopolymers and the copolymers poly(**1**-co-**3**) or poly(**1**-co-**2**) are shown in figure 3C and 3D respectively. poly(**1**-co-**3**) demonstrated excellent thermal stability with a $T_{d,10\%}$ (10% mass loss temperature) of >305 °C for copolymers with up to 49 % incorporation of **1**. Comparatively, poly(**1**-co-**3**) with 64 % incorporation of **1** had a slightly lower $T_{d,10\%}$ (287 °C), which could be attributed to the increasing content of acetal-ester units in the copolymer chain as observed previously in the copolymerization of lactide with dioxolane.[41] poly(**1**-co-**2**) demonstrated moderate thermal stability with $T_{d,10\%}$ >220 °C for all copolymers with $T_{d,10\%}$ increasing to 289 °C with 65 % incorporation of **1**. The lower thermal stability of poly(**1**-co-**2**) copolymers containing higher % of **2** could be attributed to the fragmentation of pendant

allylic ether groups in the copolymer which starts around 225 °C, as reported in literature.[45] Overall, these results exemplify that the thermal properties of levoglucosan-based copolymers can be tailored over a wide range by modifying the copolymer composition and levoglucosan pendant group.

In conclusion, we have presented a scalable synthetic platform to access levoglucosan and ε-caprolactone based copolymers with different pendant functional groups via cROCOP. Through systematic screening experiments, we identified bismuth triflate as the catalyst for cROCOP of levoglucosan under mild conditions. Our screening studies indicated successful copolymer formation from tribenzyl levoglucosan and ε-caprolactone, as well as from tribenzyl and triallyl levoglucosan derivatives. The multiple pendant allylic groups preserved in the copolymer can be easily reacted *via* post-polymerization modification to modify properties and create other polymer architectures. The copolymer composition was controlled by the feed ratio and a series of copolymers with tribenzyl levoglucosan composition ranging from 16 % to 79 % were prepared. Monomer reactivity ratio analysis indicated a predominantly gradient microstructure for levoglucosan-based copolymers. These copolymers generally demonstrated good thermal stability as well as tunable T_g (ranging from −44.3 ℃ to 33.8 ℃) and crystallization behavior based on the copolymer composition. We believe this work may stimulate the development of other sugar-based copolymers via simultaneous ring-opening polymerization chemistries for next generation sustainable and biocompatible polymeric materials.

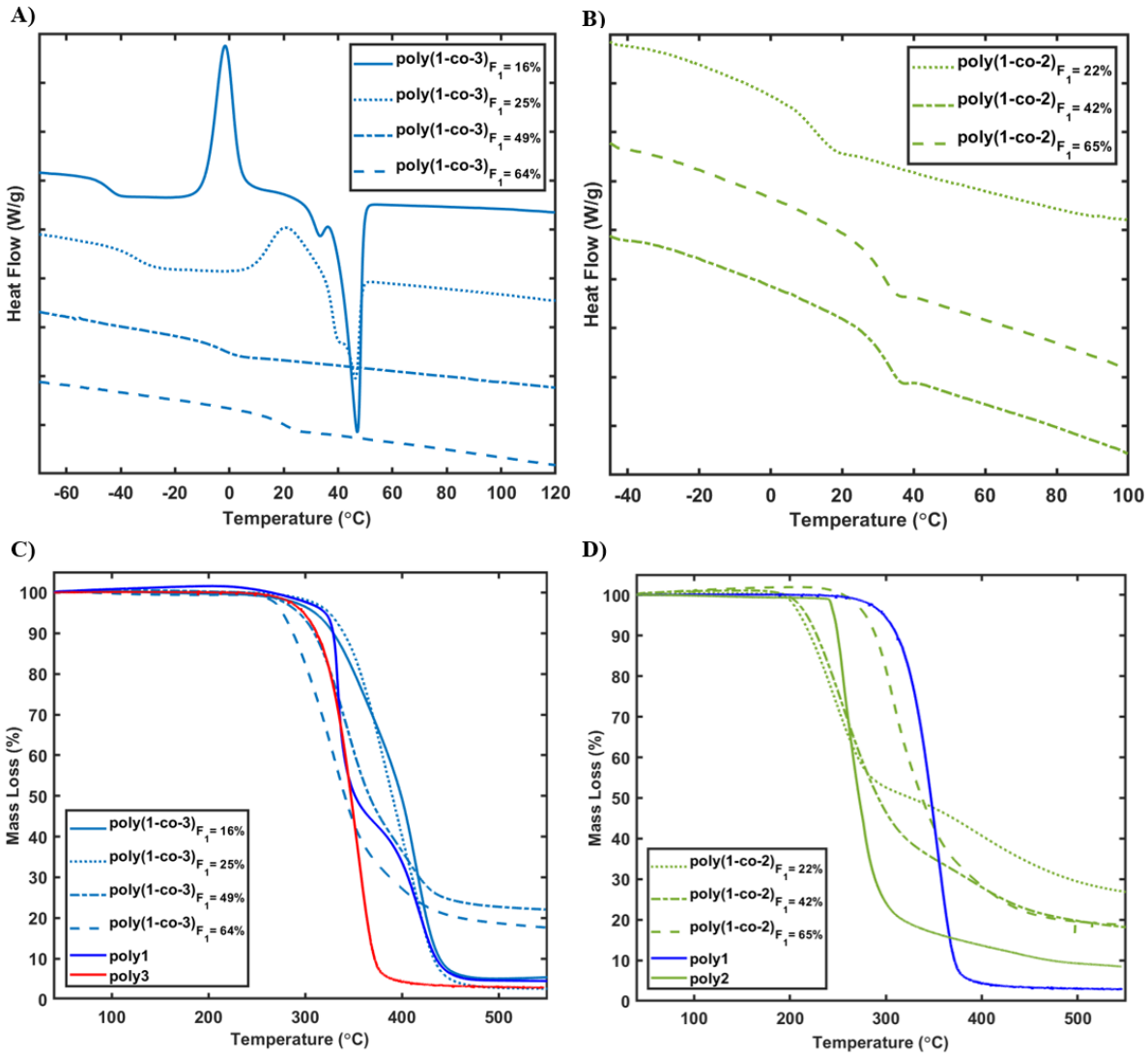

E)

Sample	T_g (°C)	T_m (°C)	T_c (°C)	$T_{d,10\%}$ (°C)
poly**1**	32	-	-	312
poly**2**	5	-	-	250
poly**3**	–60	61	34	328
poly(**1**-co-**3**) F1 = 16%	–44	28, 53	–2	330
poly(**1**-co-**3**) F1 = 25%	–31	42, 52	21	339
poly(**1**-co-**3**) F1 = 49%	–1	-	-	309
poly(**1**-co-**3**) F1 = 64%	21	-	-	287
poly(**1**-co-**2**) F1 = 22%	16	-	-	221
poly(**1**-co-**2**) F1 = 42%	33	-	-	228
poly(**1**-co-**2**) F1 = 65%	34	-	-	289

Figure 3. A) Comparison of the DSC thermograms for poly(**1**-co-**3**) with different tribenzyl

levoglucosan contents. B) Comparison of the DSC thermograms for poly(**1**-co-**2**) with different tribenzyl levoglucosan contents. C) Comparison of TGA curves for poly**1**, poly**3**, and poly(**1**-co-**3**) with different tribenzyl levoglucosan contents. D) Comparison of TGA curves for poly**1**, poly**2**, and poly(**1**-co-**2**) with different tribenzyl levoglucosan contents. E) Summary of thermal properties of levoglucosan-based copolymers.

Notes

The authors declare no competing financial interest.

Supporting Information

Experimental protocols and procedures, ^{1}H NMR spectra, reactivity ratio analysis, kinetics, conversion, DSC, SEC-MALS, DOSY NMR and data are listed.

Acknowledgments

This work was supported and funded by the NSF Center for Sustainable Polymers at the University of Minnesota; a National Science Foundation supported Center for Chemical Innovation (CHE-1901635). The authors acknowledge Emily Prebihalo for her aid in DOSY NMR. The AX-400 NMR data reported in this publication was supported by the Office of the Vice President of Research, College of Science and Engineering, and the Department of Chemistry at the University of Minnesota. The HD-500 and AV-500 NMR data reported in this publication was supported by the Office of the Director, National Institutes of Health, under Award Number S10OD011952. The content is solely the responsibility of the authors and does not necessarily represent the official views of the National Institutes of Health.

References

(1) Wang, X.; Huo, Z.; Xie, X.; Shanaiah, N.; Tong, R. Recent Advances in Sequence-Controlled Ring-Opening Copolymerizations of Monomer Chem Asian J. **2023**, 18, e202201147 (1-24). https://doi.org/10.1002/asia.202201147.

(2) Li, H.; Guillaume, S. M.; Carpentier, J. F. Polythioesters Prepared by Ring-Opening Polymerization of Cyclic Thioesters and Related Monomers. Chem Asian J. **2022**, 17, e202200641 (1-24). https://doi.org/10.1002/asia.202200641.

(3) Plajer, A. J.; Williams, C. K. Heterocycle/Heteroallene Ring-Opening Copolymerization: Selective Catalysis Delivering Alternating Copolymers. *Angew Chem Int Ed* **2022**, 61, e202104495 (1-24). https://doi.org/10.1002/anie.202104495.

(4) Longo, J. M.; Sanford, M. J.; Coates, G. W. Ring-Opening Copolymerization of Epoxides and Cyclic Anhydrides with Discrete Metal Complexes: Structure-Property Relationships. *Chem. Rev.* **2016**, 116 (24), 15167–15197. https://doi.org/10.1021/acs.chemrev.6b00553.

(5) Shen, T.; Chen, K.; Chen, Y.; Ling, J. Ring-Opening Polymerization of Cyclic Acetals: Strategy for Both Recyclable and Degradable Materials. *Macromol Rapid Commun* **2023**. https://doi.org/10.1002/marc.202300099.

(6) Shrivastava, A. Polymerization. In *Introduction to Plastics Engineering*; Elsevier, **2018**; pp 17–48. https://doi.org/10.1016/B978-0-323-39500-7.00002-2.

(7) Geyer, R.; Jambeck, J. R.; Law, K. L. *Production, Use, and Fate of All Plastics Ever Made*; **2017**. https://www.science.org.

(8) Hong, M.; Chen, E. Y.-X. Future Directions for Sustainable Polymers. *Trends Chem* **2019**, *1* (2), 148–152.

(9) Isikgor, F. H.; Becer, C. R. Lignocellulosic Biomass: A Sustainable Platform for the Production of Bio-Based Chemicals and Polymers. *Polym Chem* **2015**, *6* (25), 4497–4559. https://doi.org/10.1039/c5py00263j.

(10) Maduskar, S.; Maliekkal, V.; Neurock, M.; Dauenhauer, P. J. On the Yield of Levoglucosan from Cellulose Pyrolysis. *ACS Sustain Chem Eng* **2018**, *6* (5), 7017–7025. https://doi.org/10.1021/acssuschemeng.8b00853.

(11) Rover, M. R.; Aui, A.; Wright, M. M.; Smith, R. G.; Brown, R. C. Production and Purification of Crystallized Levoglucosan from Pyrolysis of Lignocellulosic Biomass. *Green Chemistry* **2019**, *21* (21), 5980–5989. https://doi.org/10.1039/c9gc02461a.

(12) Wang, J.; Lu, Z.; Shah, A. Techno-Economic Analysis of Levoglucosan Production via Fast Pyrolysis of Cotton Straw in China. *Biofuels, Bioproducts and Biorefining* **2019**, *13* (4), 1085–1097. https://doi.org/10.1002/bbb.2004.

(13) Kubisa, P.; Vairon, J. P. Ring-Opening Polymerization of Cyclic Acetals. *Polymer Science: A Comprehensive Reference, 10 Volume Set* **2012**, *4*, 183–211. https://doi.org/10.1016/B978-0-444-53349-4.00103-5.

(14) Wei-Ping Lin, J.; Schuerch, C.; Uryu, T.; Libert, H.; Zachoval, J.; Schuerch, C. Copolymerization of l,6-Anhydro-2,3,4-Tri-0-(p-Methylbenzyl)-β-D-Glucopyranose and l,6-Anhydro-2,3,4-Tri-0-Benzyl-β-D-Galactopyranose. Possible Application to the Synthesis of Stereoregular Heteropolysaccharides and Oligosaccharides. *Macromolecules* **1973**, 6, 3, 320–324. https://doi.org/10.1021/ma60033a003.

(15) Hiroshi, I.; Conrad, S. Synthesis of α-(1→3)-Branched Dextrans by Copolymerization and α-D-Glucosidation. *J Am Chem Soc* **1979**, *101* (19), 5797–5806. https://doi.org/10.1021/ja00513a055.

(16) Uryu, T.; Hatanaka, K.; Matsuzaki, K.; Kuzuhara, H. Synthesis Of Stereoregular Heteropolysaccharides Having Amino-Groups By Ring-Opening Copolymerization Of 1,6-Anhydro-Azido-Sugar Derivatives. *J Polym Sci A1* **1983**, 21 (8), 2203–2214. https://doi.org/10.1002/pol.1983.170210805.

(17) KobayashP, K.; Sumitomo, H. Regioselectively Modified Stereo Regular Polysaccharides, 12 a) Synthesis of (1→6)-a-Linked Polysaccharides Consisting of Dglucose and 2,3,4-Tri-O-Octadecyl-β-glucose Units. *Makromol Chem*. **1988**, 189, 1019-1026. https://doi.org/10.1002/macp.1988.021890506

(18) Kanno, K.-I.; Kinoshita, W.; Kobayashi, K.; Hatanakat, K. Synthesis of Stereoregular Polysaccharide Derivatives Carrying 2,3-Di-O-Alkyl Chains. *Polymer Journal*. **1995**, 27, 911–916. https://www.nature.com/articles/pj1995118

(19) Kobayashi, K.; Kondo, T. Synthesis of a Regiospecifically Fluorinated Polysaccharide 3-Deoxy-3-Fluoro-(1f6)-R-D-Glucopyranan via Ring-Opening Polymerization. *Macromolecules*. **1997**, 30, 21, 6531–6535. https://doi.org/10.1021/ma970691s.

(20) Han, S.; Kanematsu, Y.; Hattori, K.; Nakashima, H.; Yoshida, T. Ring-Opening Polymerization of Benzylated 1,6-Anhydro-β-D-Lactose and Specific Biological Activities of Sulfated (1 →6)-α-D-Lactopyranans m. *J Polym Sci A Polym Chem* **2009**, *47* (3), 913–924. https://doi.org/10.1002/pola.23210.

(21) Ruckel, E. R.; Schuerch, C. Preparation of High Polymers from l,6-Anhydro-2,3,4-Tri-O-Substituted β-D-Glucopyranose. *Journal of Organic Chemistry* **1966**, *31* (7), 2233–2239. https://doi.org/10.1021/jo01345a035.

(22) Uryu, T.; Hatanaka, K.; Matsuzaki, K. Copolymerization of 1,6-Anhydro-Sugar Derivatives with Cyclic Monomers, 1 Tri-O-Benzyl Ether and Tri-O-Methyl Ether of 1,6-Anhydro-β-D-Glucopyranose as Sugar Monomers. *Makromol Chem*. **1980**, 181, 2137-2149. https://doi.org/10.1002/macp.1980.021811011.

(23) Woodruff, M. A.; Hutmacher, D. W. The Return of a Forgotten Polymer - Polycaprolactone in the 21st Century. *Progress in Polymer Science*. **2010**, 35, 1217–1256.

https://doi.org/10.1016/j.progpolymsci.2010.04.002 (24) Kumar, R.; Santa Chalarca, C. F.; Bockman, M. R.; Bruggen, C. Van; Grimme, C. J.; Dalal, R. J.; Hanson, M. G.; Hexum, J. K.; Reineke, T. M. Polymeric Delivery of Therapeutic Nucleic Acids. *Chemical Reviews*. **2021**, 121, 18, 11527–11652. https://doi.org/10.1021/acs.chemrev.0c00997.

(25) Wang, Z.; Yuan, L.; Tang, C. Sustainable Elastomers from Renewable Biomass. *Acc Chem Res* **2017**, *50* (7), 1762–1773. https://doi.org/10.1021/acs.accounts.7b00209.

(26) Alam, M. M.; Jack, K. S.; Hill, D. J. T.; Whittaker, A. K.; Peng, H. Gradient Copolymers – Preparation, Properties and Practice. *European Polymer Journal*. **2019**, 116, 394–414. https://doi.org/10.1016/j.eurpolymj.2019.04.028.

(27) Higuchi, M.; Kanazawa, A.; Aoshima, S. Tandem Unzipping and Scrambling Reactions for the Synthesis of Alternating Copolymers by the Cationic Ring-Opening Copolymerization of a Cyclic Acetal and a Cyclic Ester. *ACS Macro Lett* **2020**, *9* (1), 77–83. https://doi.org/10.1021/acsmacrolett.9b00874.

(28) Kost, B.; Basko, M. Synthesis and Properties of L-Lactide/1,3-Dioxolane Copolymers: Preparation of Polyesters with Enhanced Acid Sensitivity. *Polym Chem* **2021**, *12* (17), 2551–2562. https://doi.org/10.1039/d1py00358e.

(29) Higuchi, M.; Kanazawa, A.; Aoshima, S. Unzipping and Scrambling Reaction-Induced Sequence Control of Copolymer Chains via Temperature Changes during Cationic Ring-Opening Copolymerization of Cyclic Acetals and Cyclic Esters. *Journal of Polymer Science* **2021**, *59* (22), 2730–2741. https://doi.org/10.1002/pol.20210197.

(30) Qiu, H.; Shen, T.; Yang, Z.; Wu, F.; Li, X.; Tu, Y.; Ling, J. Janus Polymerization: A One-Shot Approach towards Amphiphilic Multiblock Poly(Ester-Acetal)s Directly from 1,3-Dioxolane with ε-Caprolactone. *Chin J Chem* **2022**, *40* (6), 705–712. https://doi.org/10.1002/cjoc.202100782.

(31) Kaya, K.; Debsharma, T.; Schlaad, H.; Yagci, Y. Cellulose-Based Polyacetals by Direct and Sensitized Photocationic Ring-Opening Polymerization of Levoglucosenyl Methyl Ether. *Polym Chem* **2020**, *11* (43), 6884–6889. https://doi.org/10.1039/d0py01307b.

(32) Porwal, M. K.; Reddi, Y.; Saxon, D. J.; Cramer, C. J.; Ellison, C. J.; Reineke, T. M. Stereoregular Functionalized Polysaccharides via Cationic Ring-Opening Polymerization of Biomass-Derived Levoglucosan . *Chem Sci* **2022**, *13* (16), 4512–4522. https://doi.org/10.1039/d2sc00146b.

(33) Abel, B. A.; Snyder, R. L.; Coates, G. W. Chemically Recyclable Thermoplastics from Reversible-Deactivation Polymerization of Cyclic Acetals. *Science* **2021**, *373* (6556), 783–789. https://doi.org/10.1126/science.abh0626.

(34) Nomura, N.; Taira, A.; Tomioka, T.; Okada, M. Catalytic Approach for Cationic Living Polymerization: $Sc(OTf)_3$-Catalyzed Ring-Opening Polymerization of Lactones. *Macromolecules* **2000**, *33* (5), 1497–1499. https://doi.org/10.1021/ma991580r.

(35) Lahcini, M.; Qayouh, H.; Yashiro, T.; Weidner, S. M.; Kricheldorf, H. R. Bismuth-Triflate-Catalyzed Polymerizations of ε-Caprolactone. *Macromol Chem Phys* **2011**, *212* (6), 583–591. https://doi.org/10.1002/macp.201000517.

(36) Beckingham, B. S.; Sanoja, G. E.; Lynd, N. A. Simple and Accurate Determination of Reactivity Ratios Using a Nonterminal Model of Chain Copolymerization. *Macromolecules* **2015**, *48* (19), 6922–6930. https://doi.org/10.1021/acs.macromol.5b01631.

(37) Lynd, N. A.; Ferrier, R. C.; Beckingham, B. S. Recommendation for Accurate Experimental Determination of Reactivity Ratios in Chain Copolymerization. *Macromolecules* **2019**, *52* (6), 2277–2285. https://doi.org/10.1021/acs.macromol.8b01752.

(38) Odian, G. *Principles of Polymerization*; John Wiley & Sons, **2004**.

(39) Lee, B. F.; Wolffs, M.; Delaney, K. T.; Sprafke, J. K.; Leibfarth, F. A.; Hawker, C. J.; Lynd, N. A. Reactivity Ratios and Mechanistic Insight for Anionic Ring-Opening Copolymerization of Epoxides. *Macromolecules* **2012**, *45* (9), 3722–3731. https://doi.org/10.1021/ma300634d.

(40) Higuchi, M.; Kanazawa, A.; Aoshima, S. Unzipping and Scrambling Reaction-Induced Sequence Control of Copolymer Chains via Temperature Changes during Cationic Ring-Opening Copolymerization of Cyclic Acetals and Cyclic Esters. *Journal of Polymer Science* **2021**, *59* (22), 2730–2741. https://doi.org/10.1002/pol.20210197.

(41) Kost, B.; Basko, M. Synthesis and Properties of L-Lactide/1,3-Dioxolane Copolymers: Preparation of Polyesters with Enhanced Acid Sensitivity. *Polym Chem* **2021**, *12* (17), 2551–2562. https://doi.org/10.1039/d1py00358e.

(42) Alizadeh, A.; Richardson, L.; Xu, J.; McCartney, S.; Marand, H.; Cheung, Y. W.; Chum, S. Influence of Structural and Topological Constraints on the Crystallization and Melting Behavior of Polymers. 1. Ethylene/1-Octene Copolymers. *Macromolecules* **1999**, *32* (19), 6221–6235. https://doi.org/10.1021/ma990669u.

(43) Schick, C. Differential Scanning Calorimetry (DSC) of Semicrystalline Polymers. *Anal Bioanal Chem* **2009**, *395* (6), 1589–1611. https://doi.org/10.1007/s00216-009-3169-y.

(44) Bajpai, O. P.; Panja, S.; Chattopadhyay, S.; Setua, D. K. Process-Structure-Property Relationships in Nanocomposites Based on Piezoelectric-Polymer Matrix and Magnetic Nanoparticles. *In Manufacturing of Nanocomposites with Engineering Plastics*. **2015**, 255-278. https://doi.org/10.1016/B978-1-78242-308-9.00011-2.

(45) Vardareli, T. K.; Keskin, S.; Usanmaz, A. Thermal Degradation of Poly(Allyl Methacrylate) by Mass Spectroscopy and TGA. *Journal of Macromolecular Science, Part A: Pure and Applied Chemistry* **2006**, *43* (10), 1569–1581. https://doi.org/10.1080/10601320600896900.